*Asociación Argentina de Astronomía*
*BAAA, Vol. 47, 2004*
*P. Cincotta, G. Dubner, S. Malaroda, C.H. Mandrini, H. Muriel, G.E. Romero and R. Vázquez, eds.*
INFORME INVITADO – INVITED REVIEW

# Recent progress in observational cosmology

Alejandro Gangui
*Instituto de Astronomía y Física del Espacio,*
*Ciudad Universitaria, 1428 Buenos Aires, Argentina*
*and*
*Dept. de Física and CEFIEC, Universidad de Buenos Aires,*
*Ciudad Universitaria – Pab. 1, 1428 Buenos Aires, Argentina*
www.iafe.uba.ar/gangui.html

**Abstract.** We present here a short update of some topics on observational cosmology, with special emphasis given to the latest results on the cosmic microwave background radiation anisotropies and polarization.

**Resumen.** Hacemos un breve resumen de algunos temas de cosmología observacional, con especial atención en los últimos resultados obtenidos en observaciones de la radiación cósmica del fondo de microondas, tanto en sus anisotropías como en su polarización.

## 1. Introduction

Over the past recent years a standard model for cosmology has emerged. With a small number of parameters, this current model describes very well the evolution of the universe, since it was a tiny fraction of a second old, to the present time, and reproduces observations on scales ranging from a few to thousands of megaparsecs. The favorite cosmological model from the Wilkinson Microwave Anisotropy Probe (WMAP) data (Bennet et al. 2003) is a spatially flat universe, with Gaussian, adiabatic and approximately scale-invariant cosmological fluctuations, plus an early era of global reionization, at a redshift around $z = 20$. The estimated baryon density is no larger than a 5% of the critical density (that results in a flat Euclidean universe), with a roughly 22% contribution in dark matter and the rest in some yet unknown form of dark enery (Gangui 2003).
Many independent astrophysical observations agree within small error bars with these estimates. An example is the present value of the Hubble constant, narrowed to $71 \pm 4$ km/seg/Mpc. All this is in good agreement with what is obtained from galaxy surveys (Percival et al. 2001, Verde et al. 2002) and supernova events (e.g., Perlmutter et al. 1999), and is also in the right direction to match the $H = 72 \pm 3 \pm 7$ km/seg/Mpc inferred from the Hubble Key Project (Freedman et al. 2001). In this conference, many of the aforementioned astrophysical observations have been considered by other speakers and panels and therefore, in what follows, we will mainly focus on some of the recent findings in the cosmic microwave background anisotropies and polarization.

## 2. Anisotropies in the Cosmic Microwave Background

The Cosmic Microwave Background radiation (CMB hereafter) is a relic of the big bang, a cold bath of light just a few degrees above absolute zero that pervades the entire universe. Released when matter began to become structured, the CMB is our earliest "snapshot" of the universe. Variations (or anisotropies) in its effective temperature tell us about the size and strength of the initial seeds in the primordial plasma, those clouds of gas that clumped together under gravitational attraction and led to the birth of galaxies. Recent CMB experiments suggest that these fundamental seeds could have resulted from tiny primordial quantum fluctuations generated in the early universe during a period of ultra-rapid expansion called inflation (Garcia-Bellido 2004).

Anisotropies of the CMB are directly related to the origin of structure in the universe. Galaxies and clusters of galaxies eventually formed by gravitational instability from primordial density fluctuations, and these same fluctuations left their imprint on the CMB. Recent balloon (de Bernardis et al. 2000, Hanany 2000), ground-based interferometer (Halverson et al. 2001) and satellite (i.e., WMAP, Bennett et al. 2003) experiments have produced reliable estimates of the power spectrum of the CMB temperature anisotropies and, a couple of years ago, also the first detection of the CMB polarization field (Leitch et al. 2002, Kovac et al. 2002).

Successful models of structure formation and CMB fluctuations are based on the idea of inflation. In simplest inflationary models it is assumed that there exists a weakly coupled scalar field $\phi$, called the inflaton, which "drives" the (quasi) exponential expansion of the universe. The quantum fluctuations of $\phi$ are stretched by the expansion to scales beyond the horizon, thus "freezing" their amplitude. Inflation is followed by a period of thermalization, during which standard forms of matter and energy are formed. Because of the spatial variations of $\phi$ introduced by quantum fluctuations, thermalization occurs at slightly different times in different parts of the universe. Such fluctuations in the thermalization time give rise to density fluctuations. Because of their quantum nature and because of the fact that initial perturbations are assumed to be in the vacuum state and hence well described by a Gaussian distribution, perturbations produced during inflation are expected to follow Gaussian statistics to a high degree (Gangui et al. 1994, Gangui and Martin 2000), or either be products of Gaussian random variables. This is a fairly general prediction that has been tested currently with data from WMAP and will be tested more thoroughly in the future with the ESA–Planck Surveyor experiment.

Early on, when the observable universe was smaller and much hotter than is today, the free electron density was so high that photons could not propagate freely without being scattered by electrons. Due to these interactions, ionized matter, electrons and radiation behaved in a collective fashion and formed a single fluid, with the inertia provided by the baryons and the radiation pressure given by the photons. And this fluid supported sound waves. In fact, the gravitational clumping of the effective mass in the perturbations was resisted by the restoring radiation pressure, resulting in gravity-driven *acoustic oscillations* in both fluid density and local velocity.

As the universe expanded and ambient temperatures decreased, high-energy collisions became less and less frequent. Very energetic photons were not statis-

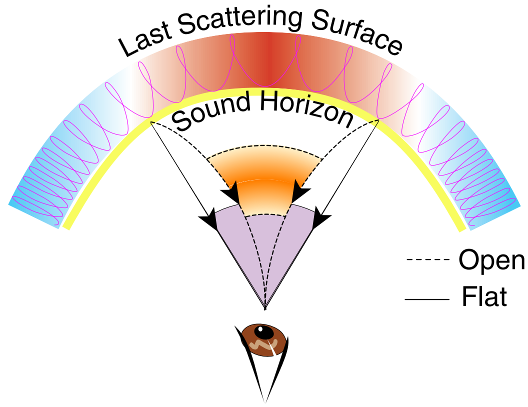


Figure 1. The angle subtended on the CMB sky today by the sound horizon at recombination depends on the various cosmological parameters. In particular, the spatial curvature of the universe will change the angle under which any feature (like the sound horizon) is seen [figure adapted from a work of Wayne Hu.]

tically significant to destroy the increasing number of neutral particles (mostly hydrogen) that began to combine. Cosmologist refer to this period as *recombination*. Soon afterwards the CMB was released free, making its *last scattering* upon matter. This is a remarkable event in the history of the universe, because it is the very moment when it passed from being opaque to being transparent to electromagnetic radiation (e.g., Gangui 2005).

Features in the radiation pattern at this time depend on the maximum distance a sound wave could have traveled since the Big Bang – the *sound horizon*. Cosmological models relate this distance to the angle $\theta$ it subtends on the sky today through the angular-diameter distance relation. This relation depends on the various unknown cosmological parameters, most importantly the total energy density in the universe. But according to Einstein's general relativity, energy implies curvature. Hence, the curvature of the universe affects the angle $\theta$ subtended today by the sound horizon at recombination (see Figure 1). For a universe devoid of spatial curvature (a flat or Euclidean geometry) models predict $\theta \approx 1^\circ$. Thus, if the universe were flat, at an angular scale of precisely $1^\circ$ we would expect to detect some characteristic feature in the CMB, the "fingerprint" of recombination.

How can this feature be detected? One convenient way of comparing theoretical model predictions with the result of observations is by means of the functions $C_\ell$, the CMB angular power spectrum of the anisotropies (something analogous is also done for the polarization field). The microwave sky is expanded into a set of functions labeled by the multipole index $\ell$. The correspondence is such that the $\ell$th multipole samples angular scales of order $\theta \sim 180^\circ/\ell$. Hence, $C_\ell$ gives us the typical strength of the temperature perturbations on that angular scale. A characteristic feature is given by the presence of peaks in the $\ell(\ell+1)C_\ell$ versus $\ell$ plot. The first *acoustic peak* in the temperature fluctuations is located at the multipole corresponding to the scale of the sound horizon at recombination, when the plasma underwent its first oscillation; it corresponds to a compression mode of the oscillating plasma.

Some years ago, the BOOMERanG collaboration announced results from the Antarctic long duration balloon flight mission of 1998 (B98). They found the first peak located at $\ell \sim 200$, at the right position for a flat universe. Only weeks later, the results from another balloon experiment, MAXIMA, were made available. MAXIMA produced high-resolution maps of a 100 square-degree patch of the northern sky and went beyond B98 in exploring multipoles from $\ell \simeq 36$ to 785, the largest range reported at that time with a single experiment.

In 2003, the WMAP collaboration published the most precise data available so far. They presented full sky microwave maps in five frequency bands (from 23 to 94 GHz) from the first year sky survey with calibration errors less than 0.5% and low systematic error levels. The CMB was separated from the foregrounds using multifrequency data, finding maps which were consistent with the 7° full-width at half-maximum COBE maps.

The WMAP team found that the CMB anisotropy obeys Gaussian statistics with a high confidence level. Their $2 \leq \ell \leq 900$ anisotropy power spectrum was cosmic variance limited for $\ell < 354$ with a signal-to-noise ratio larger than 1 per mode to $\ell = 658$. The temperature-polarization cross-power spectrum they found revealed both acoustic features and a large angle correlation from reionization. The optical depth of reionization was $\tau = 0.17 \pm 0.04$, implying a reionization epoch of $t_r = 180^{+220}_{-80}$ Myr (at 95% confidence level) after the Big Bang at a redshift of $z_r = 20^{+10}_{-9}$ (95% CL) for a range of ionization scenarios.

They performed a cosmological parameter best-fit and found a consistent cosmological model from the CMB and other measures of large scale structure. The age of the best-fit universe is $t_0 = 13.7 \pm 0.2$ Gyr old. Decoupling was at $t_{dec} = 379^{+8}_{-7}$ kyr after the Big Bang at a redshift of $z_{dec} = 1089 \pm 1$. The thickness of the decoupling surface was $\Delta z_{dec} = 195 \pm 2$. The matter density of the universe is $\Omega_m h^2 = 0.135^{+0.008}_{-0.009}$, the baryon density is $\Omega_b h^2 = 0.0224 \pm 0.0009$, and the total mass-energy of the universe is $\Omega_{tot} = 1.02 \pm 0.02$ (all data taken from Bennett et al. 2003; $\Omega_i \equiv \rho_i/\rho_c$ hereafter, where $\rho_c$ is the critical density corresponding to a spatially flat universe.

The presence of a localized and narrow ($\Delta\ell/\ell \sim 1$) peak at $\ell \sim 200$ is in agreement with a flat universe and favors an inflationary model with initial adiabatic perturbations (where fluctuations in each species are correlated). Their best candidate is a flat universe model composed of 4.4% baryons, 22% dark matter and 73% dark energy. The dark energy equation of state is limited to $w < -0.78$(95% CL). Inflation theory is supported with spectral index $n_s \approx 1$ (cf. the power-law gravitational potential primordial power spectrum $\mathrm{P}(k) \propto k^{n_s}$), $\Omega_{tot} \approx 1$, Gaussian random phases of the CMB anisotropy, and superhorizon fluctuations implied by the temperature-polarization (TE) anticorrelations at decoupling.

Even though WMAP detected a period of reionization, the acoustic peaks are not damped but clearly visible in the angular power spectrum as we know it should be from the simple physics of recombination, which predicts the existence of other peaks; the second one corresponds to a rarefaction mode and its characteristic scale is half that of the first peak. The latest data shows with a high confidence level the modulations at high multipole moments.

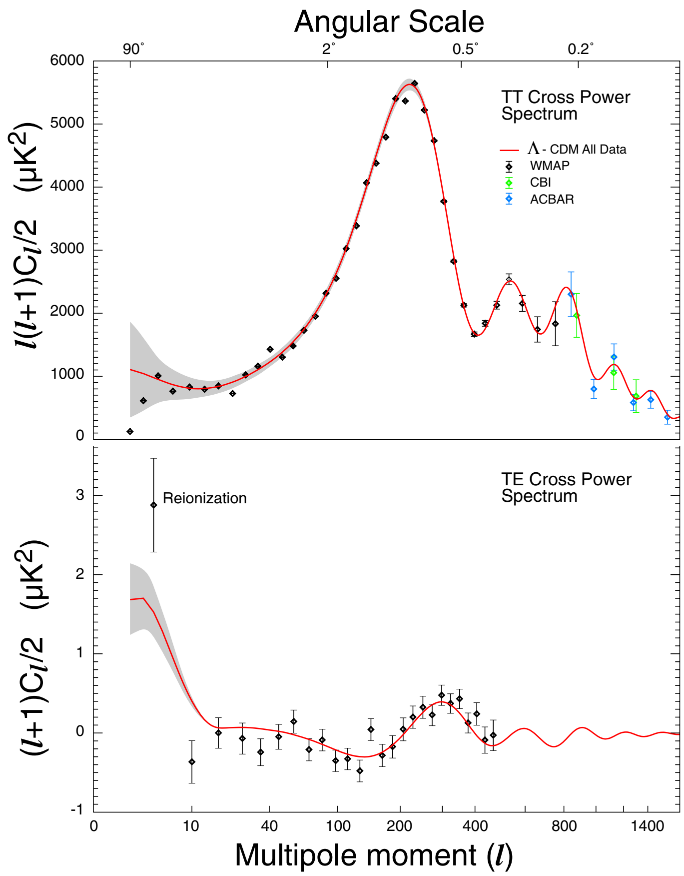


Figure 2. The WMAP angular power spectrum from Bennett et al. 2003. The upper panel shows the WMAP temperature anisotropy (TT) results, which are consistent with the ACBAR and CBI measurements. The TT angular power spectrum is highly constrained. WMAP best fit running index ΛCDM model is shown. The grey band represents the cosmic variance expected for that model. The quadrupole has a surprisingly low amplitude. There are excursions from a smooth spectrum (e.g., at $\ell \approx 40$ and $\ell \approx 210$) that are only slightly larger than expected statistically. WMAP team reports that these effects may result from a combination of cosmic variance, subdominant astrophysical processes, and other small effects from approximations made for their first year data analysis. Hopefully, this issue will be clarified with the 2-year data whose publication is imminent. At present, they do not attach cosmological significance to them. In the bottom panel we see the temperature-polarization (TE) cross-power spectrum, $(\ell+1)C_\ell/2\pi$. (We should note that this is not multiplied by the additional factor of $\ell$.) The peak in the TE spectrum near $\ell \sim 300$ is out of phase with the TT power spectrum, as predicted for adiabatic initial conditions. The antipeak in the TE spectrum near $\ell \sim 150$ is evidence for superhorizon modes at decoupling, as predicted by inflationary models.

As mentioned, the accurate locations and amplitudes of the secondary peaks has allowed the determination of many fundamental cosmological parameters and, together with other astrophysical input, such as supernovae and large scale structure data, notably from the 2dFGRS (Colless et al. 2001), the supernova cosmology project (Perlmutter et al. 1999) and the high-$z$ supernova team (Riess et al. 1998), provides a list of the "best" cosmological parameters to date (see the Table provided by the WMAP team below).

## 3. Cosmic Microwave Background Polarization

The possibility that the CMB be polarized was first discussed by Rees in 1968, in the context of anisotropic universe models. In spite of his optimism, and after many attempts during more than thirty years, including some important upper limits (e.g., Keating et al. 2001, Hedman et al. 2001), there was no positive detection of the polarization field until the DASI detection in September 2002 (Leitch et al. 2002, Kovac et al. 2002).

Unlike previous experiments, DASI reached the required sensitivity to make a sounding discovery on angular scales $\sim 0\overset{\circ}{.}5$. Along the same line, WMAP confirmed this detection with a full-sky coverage and polarization data on five different frequencies on angular scales bigger than $0\overset{\circ}{.}2$. Polarization is an important probe both for cosmological models and for the more recent history of our nearby universe. It arises from the interactions of CMB photons with free electrons; hence, polarization can *only* be produced at the last scattering surface (its amplitude depends on the duration of the decoupling process) and, unlike temperature fluctuations, it is largely unaffected by variations of the gravitational potential after last scattering[1]. Future measurements of polarization will thus provide a clean view of the inhomogeneities of the universe at about 400,000 years after the Bang.

For understanding polarization, a couple of things should be clear. First, the energy of the photons is small compared to the mass of the electrons. Then, the CMB frequency does not change, since the electron recoil is negligible. Second, the change in the CMB polarization (i.e., the orientation of the oscillating electric field $\vec{\mathrm{E}}$ of the radiation) occurs due to a certain transition, called *Thomson scattering*. The transition probability per unit time is proportional to a combination of the old ($\hat{\epsilon}_\alpha{}^{\mathrm{in}}$) and new ($\hat{\epsilon}_\alpha{}^{\mathrm{out}}$) directions of polarization in the form $|\hat{\epsilon}_\alpha{}^{\mathrm{in}} \cdot \hat{\epsilon}_\alpha{}^{\mathrm{out}}|^2$. In other words, the initial direction of polarization will be favored. Third, an oscillating $\vec{\mathrm{E}}$ will push the electron to also oscillate; the latter can then be seen as a dipole (not to be confused with the CMB dipole), and dipole radiation emits preferentially perpendicularly to the direction of oscillation. These 'rules' will help us understand why the CMB should be linearly polarized.

---

[1] With the formation of the first stars and quasars, and the subsequent UV radiation emitted by these primitive sources, the hydrogen can re-ionize. As a consequence, the CMB will scatter again upon ionized matter and will also modify its polarization, albeit on a different angular scale. As we mentioned above, data from first-year WMAP indicates that reionization did indeed take place somewhere around redshifts $z \sim 20$ (with big "error" bars), which, translated to the elapsed time since the big bang, represents roughly a few hundred million years.

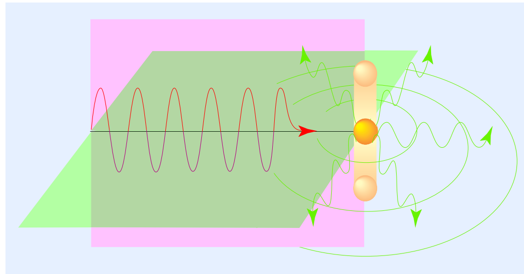

Figure 3. An electromagnetic linearly polarized wave (dark wave inciding from the left) oscillates in a given (vertical) plane. Reaching an electron (represented by a ball) the wave induces the electron to also oscillate, making it emit radiation. This resulting electromagnetic wave is concentrated essentially in the plane orthogonal to the movement of the electron and it is polarized like the incident wave.

Previous to the recombination epoch, the radiation field is unpolarized. In unpolarized light the electric field can be decomposed into the two orthogonal directions (along, say, $\hat{x}$ and $\hat{z}$) perpendicular to the line of propagation ($\hat{y}$). The electric field along $\hat{\epsilon}_{\hat{z}}^{\text{in}}$ (suppose $\hat{z}$ is vertical) will make the electron oscillate also vertically. Hence, the dipolar radiation will be maximal over the horizontal $xy$-plane. Analogously, dipole radiation due to the electric field along $\hat{x}$ will be on the $yz$-plane. If we now look from the side (e.g., from $\hat{x}$, on the horizontal plane and perpendicularly to the incident direction $\hat{y}$) we will see a special kind of scattered radiation. From our position we cannot perceive the radiation that the electron oscillating along the $\hat{x}$ direction would emit, just because this radiation goes to the $yz$-plane, orthogonal to us. Then, it is *as if* only the vertical component ($\hat{\epsilon}_{\hat{z}}^{\text{in}}$) of the incoming electric field would cause the radiation we perceive. From the above rules we know that the highest probability for the polarization of the outgoing radiation $\hat{\epsilon}_{\alpha}^{\text{out}}$ will be to be aligned with the incoming one $\hat{\epsilon}_{\hat{z}}^{\text{in}}$, and therefore it follows that the outgoing radiation will be *linearly* polarized. Now, as both the chosen incoming direction and our position as observers were arbitrary, the result will not be modified if we change them. Thomson scattering will convert unpolarized radiation into linearly polarized one.

This however is not the end of the story. To get the total effect we need to consider all possible directions from which photons will come to interact with the target electron, and sum them up. We see easily that for an initial isotropic radiation distribution the individual contributions will cancel out: just from symmetry arguments, in a spherically symmetric configuration no direction is privileged, unlike the case of a net linear polarization which would select one particular direction.

Fortunately, we know the CMB is *not exactly* isotropic; to the millikelvin precision the dominant mode is dipolar. So, what about a CMB dipolar distribution? Although spatial symmetry does not help us now, a dipole will not generate polarization either. Take, for example, the radiation incident onto the electron from the left to be more intense than the radiation incident from the right, with

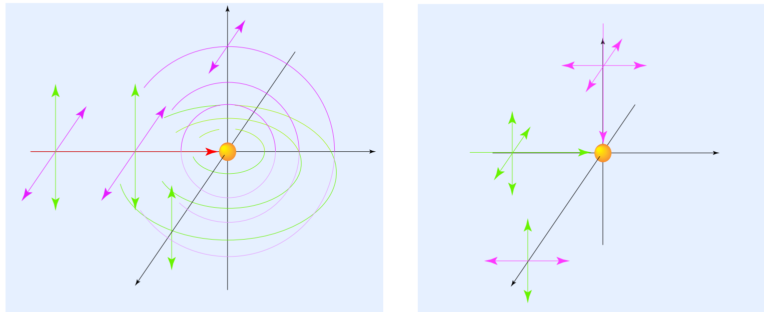

Figure 4. Left panel: non-polarized electromagnetic wave can be decomposed into the sum of two linearly-polarized waves, one along the line of sight (in dark-grey), the other along a perpendicular direction (light-grey). Scattered radiation due to the first wave is contained in the plane orthogonal to the line of sight and cannot be detected. Only the second component (in light-grey) reaches the observer and it is polarized as the incident wave. Right panel: when the charged particle receives non polarized waves from different directions, it will re-emit the radiation, polarized also along different directions, to the observer. If the original radiation is not isotropic (say, the dark-grey arrows from above are bigger than the light-grey ones from the left), then one of the resulting waves (in dark-grey) will be slightly more intense than the other, and the observer will perceive a net excess of linear polarization.

average intensities above and below (that's a dipole); it then suffices to sum up all contributions to see that no net polarization survives. However, if the CMB has a *quadrupolar* variation in temperature (that *it has*, first discovered by COBE, to tens of $\mu$K precision) then there will be an excess of vertical polarization from left- and right-incident photons (assumed hotter than the mean) with respect to the horizontal one from top and bottom light (cooler). From any point of view, orthogonal contributions to the final polarization will be different, leaving a net linear polarization in the scattered radiation.

There is one more point to emphasize. As we mentioned above, before recombination, ionized matter, electrons and radiation could be seen as forming a single fluid. In it, the inertia was provided by massive nucleons whilst the pressure was that of radiation, this interplay giving rise to acoustic waves in the density and local velocity of the fluid.

Whereas the acoustic peaks in the temperature anisotropies correspond to the compression and rarefaction maxima of the oscillating plasma, the polarization field responds to the local quadrupole moment during the decoupling process. But this local quadrupole is mainly due to the Doppler shifts induced by the velocity field of the plasma. That is why we know with certainty that polarization shows the uncontaminated dynamics of the primordial seeds at recombination.

Within standard recombination models the predicted level of linear polarization on large scales is tiny: the quadrupole generated in the radiation distribution as the photons travel between successive scatterings is too small. Multiple scatterings make the plasma very homogeneous and only wavelengths that are small enough (big $\ell$'s) to produce anisotropies over the (rather short) mean free path of the photons will lead to a significant quadrupole, and thus also to polarization. Indeed, if the CMB photons last scattered at $z \sim 1100$, the SCDM model with $h = 1$ predicts no more than 0.05 $\mu$K on scales greater than a few degrees. Hence, measuring polarization at these scales represents an experimental challenge.

However, CMB polarization increases remarkably around the degree-scale in standard models. In fact, for $\theta < 1^\circ$ a bump with superimposed acoustic oscillations reaching $\sim 5\mu$K is generically forecasted. On these scales, like for the temperature anisotropies, the polarization field shows acoustic oscillations. However, polarization spectra are sharper: temperature fluctuations receive contributions from both density (dominant) and velocity perturbations and these, being out of phase in their oscillation, partially cancel each other. On the other hand, polarization is mainly produced by velocity gradients in the baryon-photon fluid before last scattering, which also explains why temperature and polarization peaks are located differently. Moreover, acoustic oscillations depend on the *nature* of the underlying perturbation; hence, we do not expect scalar acoustic sound-waves in the baryon-photon plasma, propagating with characteristic adiabatic sound speed $c_S \sim c/\sqrt{3}$, close to that of an ideal radiative fluid, to produce the same peak-frequency as that produced by gravitational waves, which propagate with the speed of light $c$.

The main technical complication with polarization (characterized by a tensor field) is that it is not invariant under rotations around a given direction on the sky, unlike the temperature fluctuation that is described by a scalar quantity and invariant under such rotations. The level of linear polarization is conveniently expressed in terms of the *Stokes parameters* Q and U but it turns out that there is a clever combination of these parameters that results in scalar quantities (in contrast to the above noninvariant tensor description) but with different transformation properties under spatial inversions (*parity* transformations). Then, inspired by classical electromagnetism, any polarization pattern on the sky can be separated into 'electric' (scalar, unchanged under parity transformation) and 'magnetic' (pseudo-scalar, changes sign under parity) components (E- and B-type polarization, respectively). It is mainly with this new observable quantities that CMB polarization studies are performed nowadays.

## 4. Conclusions

The study of the CMB temperature anisotropies and recent detection of the CMB polarization field have been a primary tool for determining the global properties, content, and history of the universe and has led to a tremendous interest and growth in the field of precision cosmology. There is no doubt that future years, with the flow of a huge bulk of new astrophysical data, will continue to make this subject one of the most rapidly evolving ones, and allow the accurate determination of the fundamental parameters of cosmology.

**Acknowledgments**

The author thanks CONICET, UBA and FUNDACIÓN ANTORCHAS for financial support. He would also like to thank the organizers and the other participants for discusions during this interesting and charming conference.

**References**

Bennet, C. et al., Astrophys. J. Suppl. 148 (2003) 1 [arXiv:astro-ph/0302207]. Spergel et al., Astrophys. J. Suppl. 148 (2003) 175 [arXiv:astro-ph/0302209]; Peiris et al., [astro-ph/0302225]; Kogut et al., [arXiv:astro-ph/03022]

Colless, M. *et al*, Mon. Not. Roy. Astron. Soc. 328 (2001) 1039, arXiv.org:astro-ph/0106498.

de Bernardis, P. *et al.*, Nature 404, 995 (2000), arXiv.org:astro-ph/0004404.

Freedman, W., et al., Astrophys. Journal 553, 47 (2001).

Gangui, A., Science 299, 1333 (2003).

Gangui, A., *El Big Bang, la génesis de nuestra cosmología actual*, Editorial EUDEBA, Buenos Aires, 2005. (for a popular review, see for instance this book.)

Gangui, A., Lucchin, F., Matarrese, S., and Mollerach, S. *Ap. J.* **430**, 447 (1994), arXiv.org:astro-ph/9312033.

Gangui, A. and Martin, J. *Phys. Rev.* **D62**, 103004 (2000), arXiv.org:astro-ph/0001361.

Garcia-Bellido, J., The Paradigm of Inflation, arXiv.org:hep-ph/0406191.

Halverson, N., *et al*, arXiv.org:astro-ph/0104489.

Hanany, S., *et al*, arXiv.org:astro-ph/0005123; Jaffe, A.H., *et al*, arXiv.org:astro-ph/0007333.

Hedman, M., Barkats, D., Gundersen, J., Staggs, S., and Winstein, B. *Ap. J.*, **548**, L111-L114 (2001), arXiv.org:astro-ph/0010592; Hedman, M., *et al*, Astrophys. J. 573, L73 (2002).

Keating, B., *et al*, Astrophys. J. 560, L1 (2001).

Kovac, J. *et al*, Nature 420, 772-787 (2002), arXiv.org:astro-ph/0209478.

Leitch, E.M., *et al*, Nature 420, 763-771 (2002), arXiv.org:astro-ph/0209476.

Percival et al. MNRAS 327, 1297 (2001); Verde et al. MNRAS 335, 432 (2002). Bernardi, M. [arXiv:astro-ph/0303175].

Perlmutter, S., *et al*, Astrophys.J. 517 (1999) 565, arXiv.org:astro-ph/9812133.

Riess, A., *et al*, Astron.J. 116 (1998) 1009, arXiv.org:astro-ph/9805201. Riess et al., Astrophys. Journal 560, 49 (2001); J L. Tonry et al., [astro-ph/0305008].

Table 3. "Best" Cosmological Parameters

| Description | Symbol | Value | + uncertainty | − uncertainty |
|---|---|---|---|---|
| Total density | $\Omega_{tot}$ | 1.02 | 0.02 | 0.02 |
| Equation of state of quintessence | $w$ | $< -0.78$ | 95% CL | — |
| Dark energy density | $\Omega_\Lambda$ | 0.73 | 0.04 | 0.04 |
| Baryon density | $\Omega_b h^2$ | 0.0224 | 0.0009 | 0.0009 |
| Baryon density | $\Omega_b$ | 0.044 | 0.004 | 0.004 |
| Baryon density ($cm^{-3}$) | $n_b$ | $2.5 \times 10^{-7}$ | $0.1 \times 10^{-7}$ | $0.1 \times 10^{-7}$ |
| Matter density | $\Omega_m h^2$ | 0.135 | 0.008 | 0.009 |
| Matter density | $\Omega_m$ | 0.27 | 0.04 | 0.04 |
| Light neutrino density | $\Omega_\nu h^2$ | $< 0.0076$ | 95% CL | — |
| CMB temperature (K)[a] | $T_{\rm cmb}$ | 2.725 | 0.002 | 0.002 |
| CMB photon density ($cm^{-3}$)[b] | $n_\gamma$ | 410.4 | 0.9 | 0.9 |
| Baryon-to-photon ratio | $\eta$ | $6.1 \times 10^{-10}$ | $0.3 \times 10^{-10}$ | $0.2 \times 10^{-10}$ |
| Baryon-to-matter ratio | $\Omega_b \Omega_m^{-1}$ | 0.17 | 0.01 | 0.01 |
| Fluctuation amplitude in $8h^{-1}$ Mpc spheres | $\sigma_8$ | 0.84 | 0.04 | 0.04 |
| Low-$z$ cluster abundance scaling | $\sigma_8 \Omega_m^{0.5}$ | 0.44 | 0.04 | 0.05 |
| Power spectrum normalization (at $k_0 = 0.05$ Mpc$^{-1}$)[c] | $A$ | 0.833 | 0.086 | 0.083 |
| Scalar spectral index (at $k_0 = 0.05$ Mpc$^{-1}$)[c] | $n_s$ | 0.93 | 0.03 | 0.03 |
| Running index slope (at $k_0 = 0.05$ Mpc$^{-1}$)[c] | $dn_s/d\ln k$ | $-0.031$ | 0.016 | 0.018 |
| Tensor-to-scalar ratio (at $k_0 = 0.002$ Mpc$^{-1}$) | $r$ | $< 0.90$ | 95% CL | — |
| Redshift of decoupling | $z_{dec}$ | 1089 | 1 | 1 |
| Thickness of decoupling (FWHM) | $\Delta z_{dec}$ | 195 | 2 | 2 |
| Hubble constant | $h$ | 0.71 | 0.04 | 0.03 |
| Age of universe (Gyr) | $t_0$ | 13.7 | 0.2 | 0.2 |
| Age at decoupling (kyr) | $t_{dec}$ | 379 | 8 | 7 |
| Age at reionization (Myr, 95% CL)) | $t_r$ | 180 | 220 | 80 |
| Decoupling time interval (kyr) | $\Delta t_{dec}$ | 118 | 3 | 2 |
| Redshift of matter-energy equality | $z_{eq}$ | 3233 | 194 | 210 |
| Reionization optical depth | $\tau$ | 0.17 | 0.04 | 0.04 |
| Redshift of reionization (95% CL) | $z_r$ | 20 | 10 | 9 |
| Sound horizon at decoupling (°) | $\theta_A$ | 0.598 | 0.002 | 0.002 |
| Angular size distance (Gpc) | $d_A$ | 14.0 | 0.2 | 0.3 |
| Acoustic scale[d] | $\ell_A$ | 301 | 1 | 1 |
| Sound horizon at decoupling (Mpc)[d] | $r_s$ | 147 | 2 | 2 |

[a] from *COBE* (Mather et al. 1999)

[b] derived from *COBE* (Mather et al. 1999)

[c] $l_{eff} \approx 700$

[d] $\ell_A \equiv \pi\theta_A^{-1}$ $\theta_A \equiv r_s d_a^{-1}$

Figure 5. Table of the best cosmological parameters from WMAP (taken from Table 3 of Bennett et al. 2003). $\Omega_X$ is the contribution of the X component to the total density relative to the critical density; $w$ for the dark energy component comes from $p = w\rho$, with $w = -1$ for a cosmological constant $\Lambda$; $h$ is the Hubble constant in units of 100 km s$^{-1}$ Mpc$^{-1}$.